Static Stress Fatigue and Strength of a Vitreous Silicate

W. C. LEVENGOOD
The University of Michigan, Institute of Science and Technology, Ann Arbor, Michigan
(Received 15 May 1963; in final form 25 September 1963)

Various types of static loading stresses were applied to freshly cleaved surfaces formed on glass laths. With increasing applied force the number of linear flaws increased. At high stresses the number per unit area was the same order of magnitude as predicted for the pile up of surface flaws to form a microcrack. The diameter of loop flaws, originating at etch pit sources, increased with stress in agreement with a theoretical prediction based on a vacancy diffusion mechanism. It was postulated that with applied loads the vacancies diffuse into the loop source region and increase the local stress field. This stress is partially relieved by the loop expansion.

Higher flaw densities were found by etching during actual stress application than by loading in air followed by placing in the etchant. This difference was explained for samples loaded in air by the release of the stress causing some of the flaws to disappear before placing in the etchant, whereas loading under the etchant displays the flaws formed during the loading period. Probe experiments showed that the flaw patterns are not the result of a stress release effect in a surface film created by the etching solution.

Samples subjected to localized forces, applied under the etchant, disclosed an increase in local flaw concentration in direct proportion to the load. The results appeared to be linear until the typical Hertz cone fracture occurred. At fracture there was a sudden decrease in the flaws formed at the load region. This decrease in flaw concentration at fracture was believed to indicate the combining of flaws to form a microcrack.

The importance of surface energy changes on the flaw formation was also shown in quantitative measurements. With decreasing surface energy the flaw length F_l and flaw number F_n also decreased. On aged surfaces the flaw interaction is less extensive and this may explain the reported higher indentation strengths on cleavage surfaces that have been aged. The buildup of flaws and the formation of microcracks also offers a possible explanation for the maximum measured strength of glass being less than one-half the theoretical value.

I. INTRODUCTION

THE observations reported in this paper demonstrate that subtle changes resulting from static stress fatigue occur within a noncrystalline network. Silicate glasses are used in this study and a part of the experimentation relates to a more detailed investigation of a previously reported loop defect expansion.[1] It is theorized and shown experimentally that static fatigue involves defect interactions on the glass surface. The experimental observations indicate a close relationship between structure sensitive defects in glass and crack formation.

Most of the previously reported experimental work involving static fatigue in glass alludes to measuring the breaking strength as a function of the time duration of stress application, with close attention to the type of surrounding atmosphere. Historically the experimental evidence shows that in static fatigue the surface condition is an unknown but also very important parameter. The effect of the unknown surface variable has been circumvented by Mould[2] and others who used samples given severe amounts of abrasion. With this surface abrasion technique the dispersion of the static strength data was considerably reduced and many of the fatigue effects were more clearly shown. From these findings, however, it is difficult to obtain a clear understanding of what is occurring within the glass structure. In the study reported here the problem of surface variation is re-examined using a chemical etching technique for developing minute structure-sensitive flaws in glass.[3] The microscopic details of flaw interactions are quantitatively studied on surfaces that have not received major physical alterations.

The influence of the etchant on the patterns developed is also considered. It is concluded that the chemical treatment does not produce the etch patterns. The etchant only enhances the linear defect patterns to the point where they may be visually observed. Both similarities and differences in properties between the flaws in glass and dislocations in crystalline materials are delineated. This type of linear flaw appears to be a characteristic of glass, possibly resulting from the fact that glass has a unique structure in the category of solids. The interaction of these flaws under static fatigue is believed to lead to microcrack formation and may explain why the experimental strength of glass is generally observed to be less than one-third the theoretically predicted value.

II. PROPOSED STATIC FATIGUE MECHANISM

Previous studies of flaw mechanisms in glass have shown extensive defect formations produced under both dynamic and static stress conditions. Flaws have been found to be associated with fracture origins, the tips of internal cracks, scratches and indenter traces, and thermal stresses.[3,4] The relationship of these various defect formations to the actual production of a fatigue

[1] W. C. Levengood, J. Appl. Phys. **32**, 2525 (1961).
[2] R. E. Mould, J. Am. Ceram. Soc. **44**, 467 (1961).
[3] W. C. Levengood, J. Appl. Phys. **30**, 378 (1959).
[4] W. C. Levengood and T. S. Vong, J. Chem. Phys. **31**, 1104 (1959).

fracture arose as a fundamental question during the course of these studies. In this section are considered proposed mechanisms of defect interactions in glass which may lead to flaw multiplication and microcrack formation.

Admittedly there may be explanations for these effects other than those presented here; however, they are offered as an initial step toward finding the relationship between flaw formation and static fatigue. When considering the present state of knowledge concerning defect interactions one thing becomes apparent, namely, the mechanisms used to explain these phenomenon deal almost exclusively with periodic systems. The hypotheses presented in this section are to a large measure developed from theories applied to crystalline structures whereas the classic view of glass is usually presented as a "random" or nonperiodic system; however, the theories examined were in general those where the particular defect interactions being compared did not rely heavily on extensive periodicity in the network. It is shown in later sections that the extension of concepts developed from considerations of these periodic systems, disclose a high degree of compatability with the experimental observations. Aside from this pragmatic point, this approach was also felt justified for the following reasons:

1. The defect mechanisms discussed here, that is, those which refer to periodic systems, do not rely implicitly on long-range order for their operation. Basically what is required is the presence of mobile linear surface flaws with their associated Burgers vector.

2. The mobility of the linear surface flaws on glass has been demonstrated and their Burgers vector determined.[1,3,4]

3. The energy required to produce a flaw in glass is of the same order of magnitude as the energy required to create dislocations in crystals.[4]

4. Variations in the internal energy (degrees of short range order) has been recently shown in systems with systematic ionic substitutions.[5] This work suggests that glass cannot be described as a simple, random, nonperiodic system and, as a result of these localized regions of varying internal energy, defect mechanisms may operate.

5. The absence of long-range order in glass restricts flaw formation and gross movement to the surface region ($\sim$12-μ depth) rather than through the bulk of the material as in the case of dislocations in crystals. This restriction of movement is probably the primary difference between these defects.

It has been suggested that when glass is statically loaded a part of the stress energy is relieved by localized yield through the formation of the minute linear flaws.[1] When the load is removed some of these linear defects remain, and if a stress field is reapplied, new flaws are formed and they may move and interact with the existing flaws, producing cancellation or reinforcement. With increasing stress a number of flaws may reinforce or group to form a microcrack; a similar mechanism in the brittle fracture of crystals would be the pile up of climbing dislocations to produce a Griffith crack as suggested by Friedel.[6] The mechanisms in glass and crystals are, however, not identical since, as previously mentioned, flaw movement in glass is confined to the surface region.

If n flaws with Burgers vector b combine to form a microcrack on a stressed glass surface the width of the microcrack is

$$W=nb. \tag{1}$$

The stable equilibrium length of the flaws forming the microcrack is given by

$$L=n^2b/\pi K, \tag{2}$$

where K is

$$K=bG/8(1-\nu)\gamma, \tag{3}$$

with ν being Poisson's ratio, γ the surface energy, and G the shear modulus. The use of Eqs. (1) and (2) is justified by the fact that the flaws on glass move under applied stress and their Burgers vector was determined to be of the same order of magnitude ($b\simeq10^{-7}$ cm) as the value usually given for dislocations in crystals.[1] The length (L) of minimum stability of a single linear flaw was previously determined both theoretically and experimentally as

$$L\simeq5\times10^{-3}\text{ cm}. \tag{4}$$

Using $G=2.8\times10^{11}$ dyn/cm^2 and $\gamma=300$ dyn/cm we obtain $K=15.6$, and from Eq. (2), n is found to be

$$n\simeq10^2. \tag{5}$$

The width of the microcrack formed by the flaws is from Eq. (1)

$$W\simeq10^3A^0. \tag{6}$$

A crack of this width is just at the limit of visibility of the unaided eye and is much more stable than the flaws showing the sharp etch patterns. Experimentally it has been found that a microcrack etches differently than the minute surface flaws.[3] The edges of a microcrack act as nucleation sites for crystals formed during the etching (pseudomorphs of sodium-silico-fluoride) whereas the minute flaws form sharp microscopically contrasting etch lines; because of their localized stress energy, the minute flaws etch more rapidly than the lower energy microcracks. Evidence for the formation of microcracks during static fatigue is shown in a later section.

Flaw movement may be pronounced on a fresh breakage surface because of the low degree of contamination and high surface energy. Rerions have also been shown on fresh surfaces which act as sources for loop defects.[1]

[5] W. C. Levengood, J. Phys. Chem. Solids **24**, 1011 (1963).

[6] J. Friedel in *Fracture*, edited by Averback, Felbeck, Hahn, and Thomas (Technology Press, Cambridge, Massachusetts, 1959), pp. 498–523.

The origins or sources for the loop flaws etch as pits and appear to be high-stress regions. Shown in Fig. 1 is an example of a large flaw loop on a stressed breakage surface (loop origin indicated by arrow).

It is postulated that the loop sources are interstitial groupings; the justification for this postulate is the fact that under applied stress the loop sources do not indicate extensive movement. An examination of etch patterns indicates that the sources remain at relatively fixed positions in the network. With applied stress these interstitial sources may act as nucleation sites for vacancies in the glass. Energy is gained by vacancy diffusion and vacancies are destroyed by the extension of flaws at the loop source. This type of flaw extension resulting from vacancy diffusion may be defined as a type of "climb" process. Climb occurs by the very localized growth of defect aggregates and long-range periodicity is not a necessary criterion, therefore, flaw extension by climb may be a reasonable mechanism in a glass network. As pointed out by Thomson and Balluffi[7] a curvature or loop shape is introduced by the climb mechanism and this loop or curvature (Fig. 1) is a characteristic which distinguishes the loop defects in glass from the random linear flaws.

The development used to suggest how this defect mechanism operates is similar to that given by Bardeen and Herring[8] for vacancy diffusion in crystalline structures. Their concepts were, however, developed from phenomenological diffusion mechanisms where a long-range periodic structure was not the essential factor; rather gradients in chemical potential were considered to be the motivating force in the vacancy diffusion process. Many of the findings leading to their vacancy diffusion theory were based on the kinetics of defect diffusion in metal alloys (Kirkendall effect). The influence of stress was considered in terms of the concentration of vacancies and length of source associated with the dislocations or flaw loops. Variations in localized chemical potentials may also produce numerous vacancy and interstitial defects in glass systems. The systematics of vacancy and interstitial defect formation in glass have been outlined by Stevels and Kats,[9] among others. Based on these factors and the reasons previously given, the following development was believed to be justified. For the loop flaw lines to form from increases in the vacancy concentration at a loop source of length L' the condition of applied stress must be

$$\sigma > Gb/L'. \tag{7}$$

The increase in the loop diameter (D_L) gives a gain in free energy ΔF of dx per unit line length of loop flaw. The change in chemical potential at the source is related to the stress by

$$\sigma = \mu_v/\Omega_0, \tag{8}$$

where μ_v is the chemical potential and Ω_0 the atomic volume. For the flaw loops the criterion is

$$|\mu_v| > Gb\Omega_0/L'. \tag{9}$$

Bardeen and Herring show that if the number of local vacancies N_v differs from the equilibrium value N_e in the solid then

$$\mu_v = kT \log(N_v/N_e). \tag{10}$$

At a given stress equilibrium it may be seen from Eqs. (9) and (10) that

$$|\log(N_v/N_e)| = Gb\Omega_0/kTL'. \tag{11}$$

Substitution of the constants for glass; with values for other constants of $\Omega_0 \sim 10^{-23}$ cm^3, $kT = 0.4 \times 10^{-13}$ ergs and a value[10] for L' of 10^{-4} cm gives

$$|\log(N_v/N_e)| \simeq 7 \times 10^{-2}. \tag{12}$$

Equation (12) indicates that with a change in vacancy concentration of approximately seven parts in one hundred the source L' may act as an origin for loop formation. If as we have postulated, the concentration of vacancies at the source determines the loop diameter D_L, and if the loop diameter is a simple linear function of the change in concentration of the vacancies then

$$N_v/N_e = K'(D_L), \tag{13}$$

FIG. 1. Flaw loop on a stressed breakage surface, ×96.

[7] R. M. Thomson and R. W. Balluffi, J. Appl. Phys. **33**, 803 (1962).

[8] J. Bardeen and C. Herring, *Atom Movements* (American Society for Metals, Cleveland, Ohio, 1951), pp. 87–102.

[9] J. M. Stevels and A. Kats, Philips Res. Rept. **11**, 103 (1956).

[10] The size of the loop source L' was determined from detailed examination of samples given very short time etches.

where K' is a proportionality constant. After taking the logarithm of both sides of Eq. (13) the following relation between the loop diameter and the concentration of vacancies is obtained

$$\log(N_v/N_e)=C\log D_L+C', \tag{14}$$

where C and C' are constants. In terms of the corresponding stress energy as the vacancies are removed locally it is found by substitution that

$$\sigma=(kT/\Omega_0)C\log D_L+C'. \tag{15}$$

For vacancy diffusion at a source, Seitz[11] has commented that all that is necessray is to have the local concentration of vacancies a unique function of the

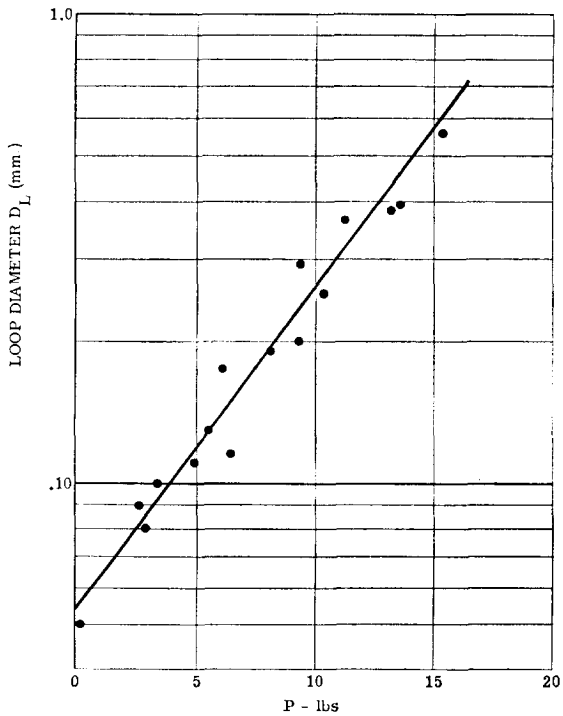

FIG. 2. Loop expansion data plotted according to Eq. (15) (shear stress).

local composition (again it appears that long-range periodicity is not essential). The local stress concentration around the interstitial loop sources could, therefore, account for the observed loop expansion with applied force.

Furthermore, the mechanism suggested in Eq. (15) could also enhance the stress gradient at the sources for spiral defect formations in glass. The spirals have been observed to form at localized nuclei[1] (interstitial groupings) and these origins may increase the local concentration of vacancies. If such a mechanism were the case one would also expect that reheating a structure containing spirals would allow gross diffusion of the vacancies out of the region and reduce the local stress field.

[11] F. Seitz, Acta Cryst. 3, 355 (1950).

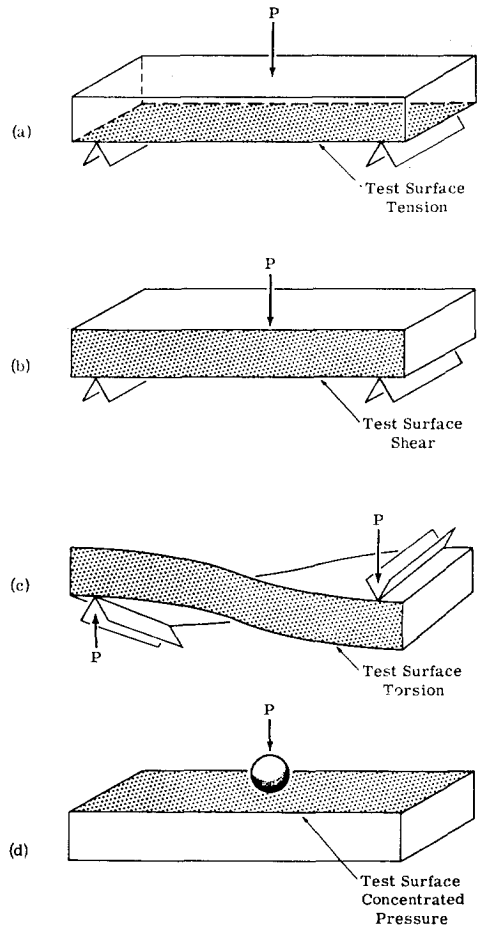

Fig. 3. Schematic representations of loading methods.

This reduction in the stress has been indicated in experiments which showed a reduction in the number of spiral regions with continued remelting.[12]

Equation (15) also makes the important prediction that the log of loop diameter D_L increases as a linear function with applied stress. This prediction is confirmed in Fig. 2, which is previously published loop expansion data (see Fig. 9 of Ref. 1), replotted according to Eq. (15). Each point is the average loop diameter (D_L) of over 30 sources measured on fresh surfaces under shear stress [Fig. 3(b)]. This curve, along with additional results to be presented in later sections, provides experimental corroboration of the vacancy diffusion mechanism proposed to explain the growth of the flaw loops with applied stress.

III. EXPERIMENTAL TECHNIQUES

Most of the flaw and loop interactions were observed on fresh breakage surfaces produced from strips of clear container glass (soda-lime–silica). This type of glass was used because the flaws and loops are easily seen

[12] W. C. Levengood and T. S. Vong, J. Appl. Phys. 31, 1416 (1960).

and microscopically studied. Each series of load samples was obtained from groups of containers similar in composition. Various types of static load stresses were applied to the test surfaces as follows:

1. Beam Loading. Simple, two-point beam loading was given 3.2-mm-thick, approximately 76-mm-long, and 12.7-mm-wide strips of glass. In some series the breakage surface was placed under tension [Fig. 3(a)] and in others the freshly exposed surface was normal to the maximum tension. These latter surfaces were designated as having a shear type of loading as shown schematically in Fig. 3(b). Simple beam loading formulas were used when calculating the applied stresses.

2. Torque Stresses. Torsion loads [Fig. 3(c)] were produced by clamping samples in a torque device used for determining magnitudes of twist. This device is calibrated directly in inch-pounds torque.[13] Samples 6.4 cm long were positioned vertically and a long C clamp secured at the top edge to act as a grip. One torque cycle consisted of a twist both in the left and right directions of equal magnitude. Although this technique is crude, a given torque treatment could be reproduced to within about 2.3 kg·cm.

3. Concentrated Forces. High static stresses were created in localized regions by pressing steel balls into the surface as shown in Fig. 3(d). The force was applied vertically to the fresh surfaces.

Flaw counts and loop diameter measurements were made at approximately ×100 magnification. The loop sizes were determined to ±0.001 mm by using a calibrated ocular micrometer. The samples were treated with the etchant, used for soda-lime–silica glasses.[3]

In the following sections several series of experiments are described where loads were applied as the samples were being etched. At this point it, therefore, appears worthwhile to discuss the influence of the etchant solution on the defect patterns. It has been suggested that the etchant may form a very thin, uniform tension film on the glass surface and that the resulting flaws, particularly the spiral patterns, may be a result of some mechanical stress release effect in this tension film. Such a proposed concept would of course not explain the creation of complex flaw patterns and the distortion of spiral regions by mechanical stresses applied to the surface *before* placing the sample in the etchant.

Although exhaustive experimentation initially indicated that the etchant solution does not create the defects, this recently suggested tension film effect was examined experimentally. Both spiral and nonspiral containing glasses were placed in the etchant and localized stresses applied after various time intervals (1-, 3-, 7-, and 10-min etching times). Vertical and torque stresses were created on fresh breakage surfaces by probing with a microspade. After probing, the samples were left in the solution for a 15-min total etching time. This microspade technique was previously found to create spiral sources at a torque stress region formed *before* placing the samples in the etchant.[12]

These probe experiments showed that in no case was there a stress release effect or the creation of spiral flaws by rupturing a tension film. Some flaw patterns, as expected, were seen around the load regions, however, their appearance was similar to flaws created by applying probes in air *before* placing in the etchant. It was interesting to note, however, that stresses applied to surfaces after being in the solution for several minutes (7 to 10 min) had less effect on moving the existing flaws than stresses applied after 1- and 3-min etching. After the longer etching times a second set of flaws was formed. The flaws created during the initial cleavage appeared to become "fixed" by the etchant and would no longer move under the applied local stress. The effect is one of new stress flaws interacting with immobile existing flaws and not, as previously mentioned, a stress release effect. The presence of two sets of flaws also rules out a sudden stress release in a film produced during the etching. From these and the previous studies we may conclude that the etchant does not produce flaw patterns; it merely displays them. The probe experiments also predict that loading under the etchant would disclose a greater flaw buildup as new flaws continuously interact with those fixed or pinned by the etchant, and it is shown later that this prediction is confirmed by experiment.

IV. LOADING RESULTS

A. Tension Stresses

Fresh breakage surfaces loaded as shown in Fig. 3(a) disclosed growth or extension of both the linear and loop type flaws with applied stress. The increase in linear flaws is shown in Fig. 4 using two different load conditions. In the case of the samples loaded in air, the load was removed after 1 min then the sample was im-

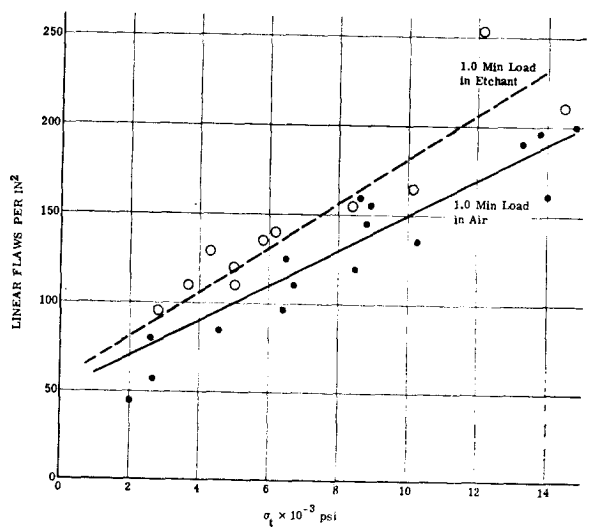

FIG. 4. Linear flaw buildup on surfaces under tension.

[13] "O. I. spring torque tester" calibration, 0–29 kg·cm.

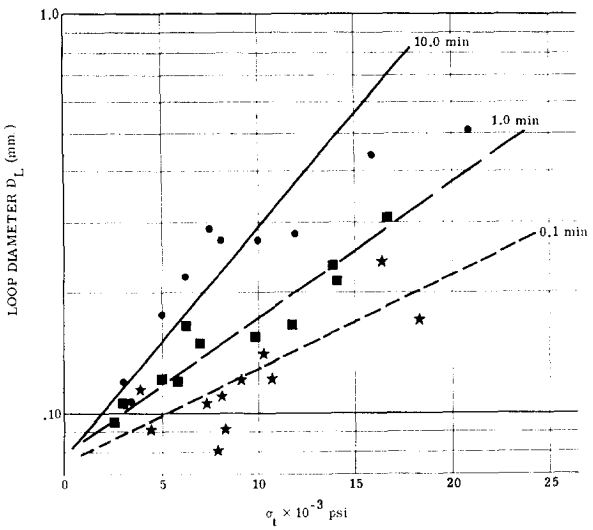

FIG. 5. Flaw loop expansion on surfaces loaded under tension in air.

mediately placed in the etchant for 15 min. With the samples loaded under the etchant the load was removed after 1 min and the test sample left in the etchant for the remaining 14 min. The linear flaws were counted in a 5.1×0.32-cm section in the stress region; loop flaws originating at a definite source were not included in these counts. Although there is considerable scatter in the individual load samples, the flaw increase with stress is apparent.

The samples loaded under the etchant for 1 min disclosed a slightly greater number of flaws than the samples loaded 1 min in air, and this appears to be due to pinning and flaw interaction on the stressed surface as shown in the probe tests. Also, in the case of the samples loaded in air, the load was released then the strip was placed in the etchant and this would account for the disappearance of a part of the flaws when the stress was removed. In the etchant the flaws become accentuated and fixed in position during the loading period and fewer disappear when the load is removed. It is also shown in Fig. 4 that at the high stresses the flaw number is of the order of magnitude given by Eq. (5) for microcrack formation.

The flaw loop expansion on surfaces loaded in air is shown in Fig. 5 for three different loading times. Each point is the average of around 30 loops on each individual sample. The scatter in Fig. 5 is pronounced and, in fact, appears to be more evident when using tension loading [Fig. 3(a)] than loading in shear [Fig. 3(b)] as may be seen by comparing the results in Fig. 5 with those in Fig. 2. Even though there is considerable scatter in the points in Fig. 5, plotting the data according to Eq. (15) produces a general random distribution of points along the lines drawn through the groups.

Two possible mechanisms may be tentatively used to explain the flaw extension results shown in Fig. 4 and 5; one is based on a previously proposed mechanism of stress release by the formation of localized regions of slip or bond readjustment.[1] In the case of the loop expansion effect in Fig. 5 a vacancy diffusion mechanism may increase the local stress field as discussed in Sec. II. In general, however, it is believed that the applied stress is relieved by the extension of both linear and loop flaws.

As a second alternative explanation, the more extensive formation of flaws on aged stressed surfaces may be conceived of as a stress release effect in a film of reaction products which forms through adsorption of water vapor, carbon dioxide, etc., on the chemically active surface. The same reasoning might be applied for this process as was suggested for the buildup of a stressed layer in the etchant. That is, as the stressed surfaces age the film depth increases and the flaw and loop growths become more pronounced.

This second explanation for the effects in Fig. 4 and 5, which is based on the influence of a surface film or contamination layer, was shown to be invalid. The change in surface energy on fresh breakage surfaces may be quantitatively shown by using the dynamic spherical indenter technique previously described in detail.[1] Fresh breakage surfaces were prepared from a base stock of samples and were aged in air for various lengths of time after which the indenter was applied (500-g load) and the flaw parameters determined. The flaw length measurements (F_1) on the aged series are shown in Fig. 6 (each point is an average of more than 30 flaw length measurements) and the decrease in flaw length with decreasing surface energy is apparent. It is found that the flaw number parameter (F_n) also decreases with aging in air. This is opposite to the effect one would expect if surface contamination were valid explanation for the flaw extension results shown in Figs. 4 and 5. From this it appears that the initially proposed release of stress by localized regions of bond readjustment or shear is a more logical mechanism.

B. Shear Stress

It is found that localized surface discontinuities may act as sources for loop formation. When a fresh breakage surface is produced it often happens that undulations in the fracture plane produce sharp macroscopic discontinuities in the fracture plane. These visible undulations are generally referred to as "rib marks." At

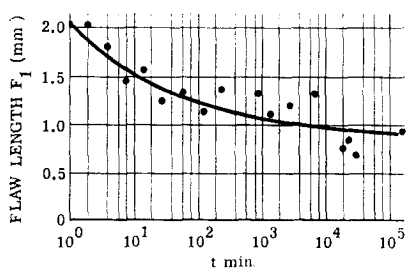

FIG. 6. Effect of aging breakage surfaces in air on flaw lengths (dynamic spherical indenter, 500-g load).

FIG. 7. Loop flaw originating at a rib mark, ×47.

the tips of these visible discontinuities the shear stresses may be high during the breaking process. It is observed that in some cases the terminus of these rib marks serve as nuclei for loop formations as shown in Fig. 7.

A series of samples with rib marks were loaded for 10-min intervals in the etchant with the fresh breakage surfaces under shear [Fig. 3(b)] and the loop diameters determined at both rib marks and at the regular nucleation sites. The results in Fig. 8 show that the loop expansion under applied stress is more pronounced at the tips of the rib marks. The stress concentration factor appears to be greater at the ends of these surface discontinuities. Each point in Fig. 8 is the average of approximately 30 sources and both curves follow the Eq. (15) relationship.

C. Torque Loading

A twist applied to the test surface [Fig. 3(c)] produces a complex stress field and the loop expansion shown in Fig. 9 does not follow the Eq. (15) prediction.

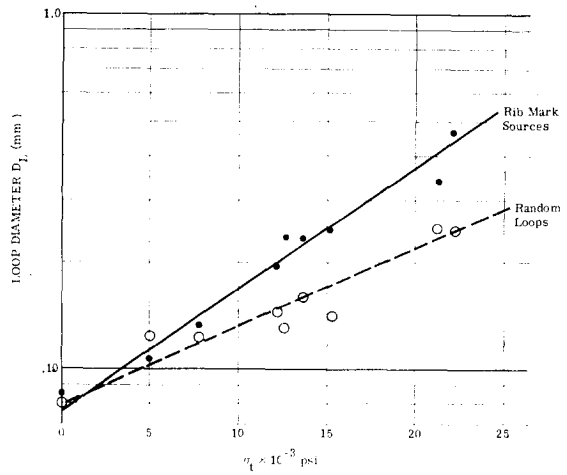

FIG. 8. Comparison of flaw loop growth from two different sources on shear surfaces (σ_t is applied tension stress).

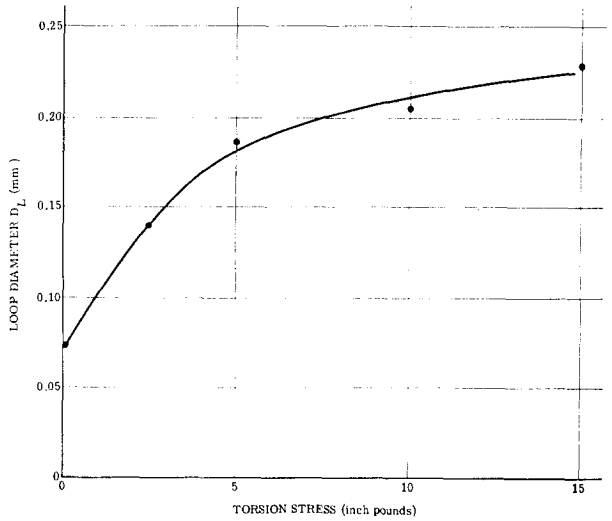

FIG. 9. Growth of flaw loops with torsion stress.

The rate of loop expansion is more rapid at the low torque stresses than at high loads. Each point on the curve in Fig. 9 represents the average diameter of over 30 loop sources on samples given 10 load cycles in air immediately after producing the fresh surface. The effect of number of torque cycles on the loop expansion is shown in Fig. 10 for full stress cycles upper curve and for half-cycles (twisted in air only to the right or left) shown in the lower curve. The applied load was 5-in. lb torque. It may be seen that with the full load cycle the loop expansion is greater than with the half stress cycles.

D. Localized Stresses

The growth and flaw multiplication with applied bending and torque stresses indicate that flaws could combine to form microcracks before the actual breakage occurs. This flaw buildup may be studied in greater detail by applying a steel ball indenter to fresh breakage surfaces [Fig. 3(d)] and observing the defect patterns in the localized stress region. A vertical force was applied at the center of areas 1.9×0.32 cm in size with the fresh surface under the etchant during the entire 15-min loading period. Loading under the etchant allows observation of the flaw patterns produced during the actual stressing, whereas loading then etching shows

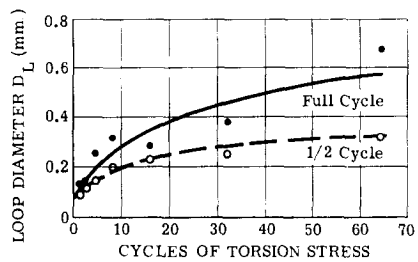

FIG. 10. Influence of torsion stress cycling on flaw loop growth.

only the final defect patterns existing after the load removal.

The number of flaws was determined in the test areas and Fig. 11 shows the results of plotting these flaw numbers as a function of the applied load (P) on a 0.64-cm steel ball. Each point is the average of flaw counts on two samples. Using a log–log plot the results appear to be linear. Similar results are shown in Fig. 12 using a 0.32-cm-diam steel ball. In this case the force was increased until a Hertz cone fracture was produced and as indicated by the arrow in Fig. 12, when fracture occurred there was a sudden decrease in the number of flaws on the test surface. It appears that the stress energy was relieved by the actual gross breaking of bonds instead of producing localized yield or flaws around the load point. A similar effect was previously shown in published photomicrographs of flaws in recovery regions after high load stresses in air.[4] As in the case here, when fracture occurred the flaw formation was less pronounced. It is also seen from Fig. 12 that at the point of fracture the flaw density is about 75 per cm^2, which is of the order of magnitude predicted by Eq. (5) for microcrack formation.

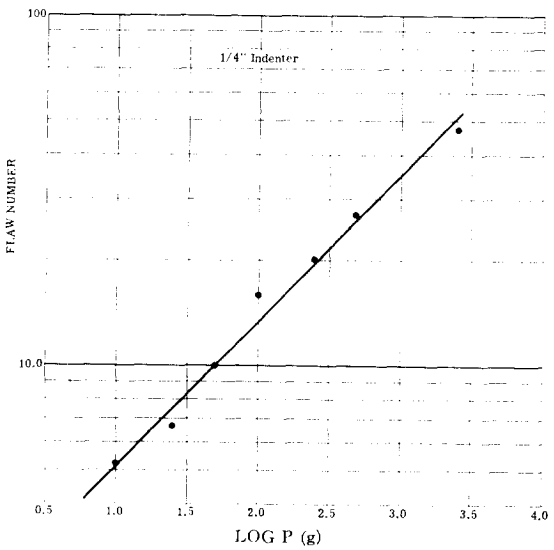

FIG. 11. Flaw formation under static loading [flaw number in 1.91-×0.32-cm area].

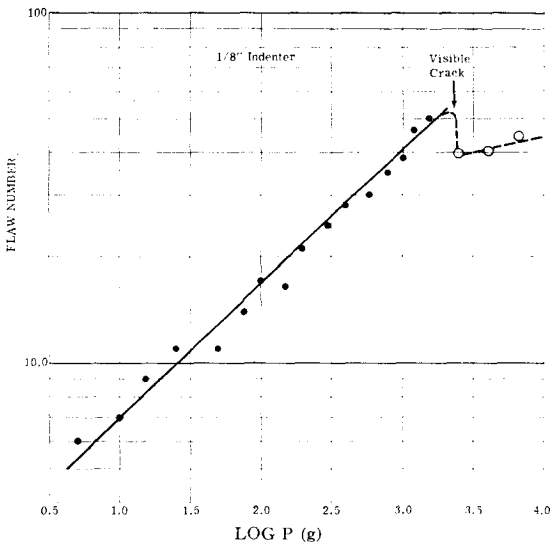

FIG. 12. Variation in flaw formation with crack formation [flaw number in 1.91-×0.32-cm area].

existing flaw patterns were in many regions broken up into groupings of short segements as shown in Fig. 13. The flaw movement was restricted to rather localized regions and this suggests a lower surface energy. These flaw interactions are also more extensive in regions where, because of the particular design of the container, thickness transitions were present; for example, the region in Fig. 13 is in an area approximately 0.32 cm wide between two sections with over 0.75-mm thickness difference. The flaw interactions as shown here were not seen on sections with no applied stress. Even though the flaw interactions are on the tension surface a pronounced component of shear stress would be present in this thickness transition region. This shear component in the stress is also indicated in Fig. 14 showing details of flaw lines in a thickness transition region. When the segments become short, as shown in the line at the

E. Qualitative Fatigue Effects

The influence of flaw interactions on static fatigue strength was also observed in a more qualitative manner on the regular commercial surfaces of laths of glass in tension [Fig. 3(a)]. The samples were cut from clear containers which were approximately 24 h old, therefore, the weathering and reaction products were not severe enough to cover over the initial flaw patterns.

On these samples the surface energy appeared to be lower than on fresh breakage surfaces. Under stress the

FIG. 13. Breakup of flaws on a commercial surface loaded in tension, ×35.

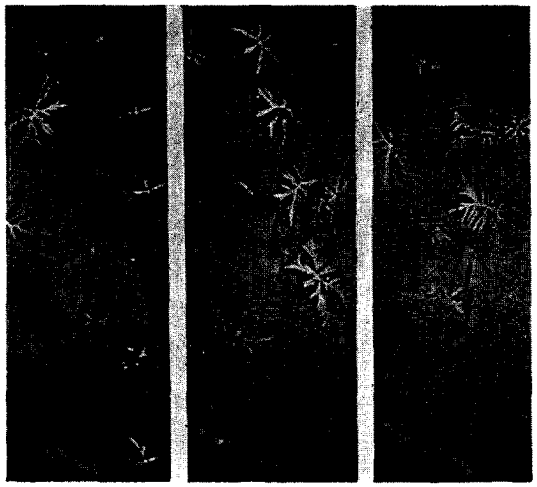

FIG. 14. Detail of flaws in regions with components of shear stress, ×64.

right in Fig. 14, they collapse into the point defects. This flaw buildup between regions of different thickness may explain the so called "hinge breakage" effect which is known to occur in impacted glass, with the origin of fracture at regions with pronounced thickness difference. From what has been shown in the preceding sections it would not be unreasonable to expect a microcrack to form more readily in the regions of thickness transition.

V. DISCUSSION OF RESULTS

In a recent paper by Sucov[14] on a discussion of ball indentation strength, it was stated that "it has been impossible thus far actually to see these flaws in glass." In this case "these flaws" refers to Griffith cracks or surface flaws.[15] In a publication[4] issued approximately three years before Sucov's statement it was shown that minute flaws were associated with localized stresses created by steel ball indenters. These flaws were shown to be more extensive at high applied loads and elastic recovery effects were also discussed.

This point is mentioned because it is felt that until workers studying these phenomenon realize that the flaws are not only present but may move and interact under applied stress, the basic fatigue mechanisms in glass cannot be completely understood. In the preceding sections it has been shown that flaw growth and buildup occurs with applied stress. By using a steel ball indenter the flaws were shown to be intimately associated with the actual breaking mechanism. The results indicate that the flaws may combine to form a microcrack preceding the gross fatigue failure of the network. This concept of flaw formation below the critical breaking stress was proposed by Poncelet[16] using an atomistic model. Poncelet's model also described the formation of flaws in brittle solids by a process of elastic flow.[17] Upon release of an applied stress a limited, reverse elastic flow may take place. Such a partial recovery could explain the lower flow density in samples where the load was removed before placing in the etchant compared with samples loaded and etched simultaneously.

Orowan[18] has expressed the idea that changes in surface energy may be responsible for static fatigue. This hypothesis appears to be well substantiated in the work reported here. It was shown, for example, that flaw formation and growth is extensive on fresh surfaces. Under controlled loading conditions a decrease in average flaw length was noted as surfaces aged in air (decreasing surface energy). On aged surfaces one might expect less flaw buildup and interaction and consequently a lower probability of microcrack formation and breakage. This hypothesis is substantiated in the indentation strength tests of Argon, Hori, and Orowan.[19] These investigators found that the indentation strength of the cleavage surfaces on a glass plate increased after aging in air for several days. In this case the reaction products on the cleavage surface may have inhibited flaw interaction and microcrack formation. Surface contamination is also known to effect dislocation motion and the mechanical yield properties of alkali halide crystals.[20]

A static fatigue mechanism based on the buildup of flaws to form a microcrack also explains the fact that the maximum observed strength of around 3×10^5 psi is less than one third the theoretical strength estimated from the bond strength of glass. Even though flaw formation allows yield, the buildup of flaws in localized regions and the ultimate formation of a microcrack prevents the stresses from reaching the theoretical bond strength of the material. For example, the stress at the point of fracture in Fig. 12 was calculated to be (using the ball contact area) approximately 2.5×10^5 psi and this is approximately at the experimentally observed limit.

The rate at which the flaws build up may also influence the breaking strength. For example, Baker and Preston[21] found strength increases in glass samples loaded for short durations and these results may be explained by a lower flaw density in samples loaded for very short intervals ($\sim$10 msec). The surrounding atmosphere also has a pronounced effect on crack growth[22] and static fatigue effects [excellent summary by O. L. Anderson in *Fracture* (Ref. 6, p. 331)]. Varia-

[14] E. W. Sucov, J. Am. Ceram. Soc. **45**, 214 (1962).
[15] A. A. Griffith, Phil. Trans. Roy. Soc. (London) **A221**, 163 (1920).
[16] E. F. Poncelet, Metals Technol. 11, Tech. Pub. 1684 (April 1944).
[17] E. F. Poncelet, Colloid Chem. **6**, 77 (1945).
[18] E. Orowan, Nature **154**, 341 (1944).
[19] A. S. Argon, Y. Hori and E. Orowan, J. Am. Ceram. Soc. **43**, 86 (1960).
[20] D. R. C. Westwood, Phil Mag. **7**, 633 (1962).
[21] T. C. Baker and F. W. Preston, J. Appl. Phys. **17**, 170 (1946).
[22] W. C. Levengood and W. H. Johnston, J. Chem. Phys. **26**, 1184 (1957).

tions in the test atmosphere would influence the surface energy (on freshly formed surfaces) and in turn the flaw formation as demonstrated by the results in Fig. 6. These intriguing and complex flaw-surface energy interactions are, however, left for future study. It is also predicted from these studies that static fatigue strength is dependent on the type of flaw structure and is related to the manner in which flaws form. A study is now in progress to investigate the relation between the previously discussed parameters of flaw length and number, and the breaking strength of the material.

ACKNOWLEDGMENTS

The author would like to express his appreciation to William Wolfe, at The University of Michigan, for helpful criticisms, and to R. A. Gaiser, Director of Research, Ball Brothers Research Corp., Muncie, Indiana, for allowing portions of this paper to be released for publication.

JOURNAL OF APPLIED PHYSICS VOLUME 35, NUMBER 2 FEBRUARY 1964

Growth of Single-Crystal Garnets by a Modified Pulling Technique

R. C. LINARES*

Bell Telephone Laboratories, Incorporated, Murray Hill, New Jersey

(Received 21 February 1962; in final form 7 June 1962)

Yttrium iron garnet has been grown by a modified pulling technique where a $BaO \cdot 0.6B_2O_3$ solvent is used instead of the pure melt. Excess garnet is taken into solution at the hotter bottom of the crucible and deposited on the cooler seed at the surface. The rate of seed rotation, the rate of withdrawal from solution, and the orientation dependence are discussed.

SINGLE crystals of yttrium iron garnet have been grown from molten salt solution[1–3] by hydrothermal techniques[4] and from melts of the component oxides.[5–7] These techniques so far have not produced large crystals having a high degree of perfection. Crystals have been grown by seeding molten salt solutions and obtaining growth by slow cooling or by transfer growth in a gradient.[8] However, these methods have not provided continuous growth over long periods of time, thus limiting the size of the crystals obtainable. The technique described herein can promote continuous growth and has been employed to produce crystals with a marked improvement in size and perfection. In this technique garnet nutrient is dissolved and transferred from the hotter region of a crucible through a molten salt solvent to a seed at the cooler surface. The seed is rotated rapidly and withdrawn slowly from the solution as growth occurs[9]

EXPERIMENTAL

For this work a 15-cm-high × 7.5-cm-diam platinum-wound tube furnace was used (Fig. 1). The bottom was closed for a distance of 6.3 cm with a brick plug and the top was closed with a removable 0.6-cm-thick zirconia cover. The furnace was controlled by cycling 10% of the voltage with a Wheelco Capacitrol. By placing the control thermocouple on the furnace windings, temperature fluctuations of no more than ±2° were obtained in the solution. The crystal pullers were capable of rotation rates up to 400 rpm and pulling rates from 25 μ per day to 0.6 cm/h. The crucibles were standard 100-ml platinum crucibles. The seed was attached to

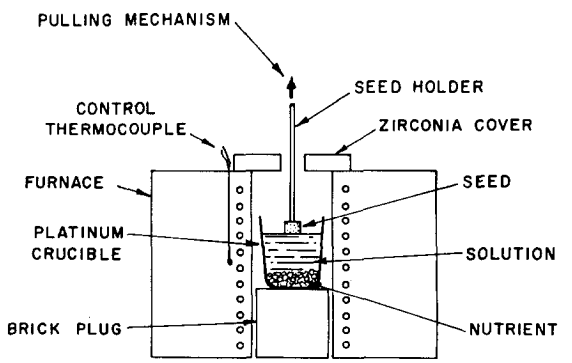

FIG. 1. Pulling furnace with crucible.

* Present address: Solid State Materials Corp., A Perkin-Elmer Subsidiary, Norwalk, Connecticut.

[1] J. W. Nielsen, E. F. Dearborn, J. Phys. Chem. Solids **5**, 202 (1958).

[2] J. W. Nielsen, J. Appl. Phys. **31**, 515S (1960).

[3] R. C. Linares, J. Am. Ceram. Soc. (to be published).

[4] R. A. Laudise, J. H. Crocket, and A. A. Ballman, J. Phys. Chem. **65**, 359 (1961); R. A. Laudise and E. D. Kolb, J. Am. Ceram. Soc. **45**, 51 (1962).

[5] E. Buehler, M. Tanenbaum (unpublished work).

[6] J. Van Hook, Fall Meeting of the Basic Science Division, American Ceramic Society, 9 October 1961.

[7] R. G. Rudness, R. W. Kebler, J. Am. Ceram. Soc. **43**, 17 (1960); L. L. Abernethy and T. H. Ramsey, Jr., J. Appl. Phys. Suppl. **32**, 376 (1961).

[8] R. A. Laudise, R. C. Linares, E. F. Dearborn, J. Appl. Phys. Suppl. **33**, 1362 (1962).

[9] F. Trumbore and E. Probansky have demonstrated the usefulness of this technique to grow alkali and rare-earth tungstate single crystals.[10]

[10] F. A. Trumbore, II, E. M. Porbansky, J. Electrochem. Soc. **109**, 94C (1961).